Observations of solar spectral irradiance change during cycle 22 from NOAA-9 Solar Backscattered Ultraviolet Model 2 (SBUV/2)

Matthew T. DeLand and Richard P. Cebula
Science Systems and Applications, Inc. (SSAI), Lanham, Maryland, USA

Ernest Hilsenrath
NASA Goddard Space Flight Center, Greenbelt, Maryland, USA

Received 14 August 2003; revised 21 January 2004; accepted 2 February 2004; published 17 March 2004.

[1] The NOAA-9 Solar Backscatter Ultraviolet Model 2 (SBUV/2) instrument is one of a series of instruments providing daily solar spectral irradiance measurements in the middle and near ultraviolet since 1978. The SBUV/2 instruments are primarily designed to measure the stratospheric profile and total column amount of ozone, using the directional albedo as the input to the ozone retrieval algorithm. Almost all optical components are common to both radiance and irradiance measurements, whose ratio forms the directional albedo, so that most response changes cancel out. As a result, the SBUV/2 instrument does not require onboard monitoring of time-dependent sensitivity changes for production of ozone data. We use vicarious comparisons with coincident Shuttle SBUV (SSBUV) solar irradiance measurements during 1989–1996, combined with observed calibration drift during the solar activity minimum in 1985–1986, to determine the long-term instrument characterization for NOAA-9 SBUV/2. This approach allows us to derive more accurate solar spectral irradiances for the period from March 1985 to May 1997, spanning two solar cycle minima with a single instrument. The NOAA-9 irradiance data show an amplitude of approximately 9.3% at 200–205 nm for solar cycle 22. This is consistent with the result of $\Delta F_{200-205}$ = 8.3% for cycle 21 from Nimbus-7 SBUV and $\Delta F_{200-205}$ = 10% for cycle 23 from UARS SUSIM. NOAA-9 data at 245–250 nm show a solar cycle amplitude of ~5.7%. The observed irradiance change at 200–205 nm between the minima of solar cycles 21 and 22 is not consistent with the UV irradiance change expected from the total solar irradiance trend suggested by *Willson and Mordvinov* [2003]. NOAA-9 SBUV/2 data can be combined with data from other instruments to create a 25-year record of solar UV irradiance. *INDEX TERMS:* 1650 Global Change: Solar variability; 7538 Solar Physics, Astrophysics, and Astronomy: Solar irradiance; 7549 Solar Physics, Astrophysics, and Astronomy: Ultraviolet emissions; 2162 Interplanetary Physics: Solar cycle variations (7536); *KEYWORDS:* solar ultraviolet irradiance, solar variability, solar cycle

Citation: DeLand, M. T., R. P. Cebula, and E. Hilsenrath (2004), Observations of solar spectral irradiance change during cycle 22 from NOAA-9 Solar Backscattered Ultraviolet Model 2 (SBUV/2), *J. Geophys. Res.*, *109*, D06304, doi:10.1029/2003JD004074.

1. Introduction

[2] Solar ultraviolet (UV) irradiance is the primary energy source for Earth's middle atmosphere, with most of the radiation in the wavelength range 190–300 nm deposited between 30 and 50 km [*Meier*, 1991]. A variety of recent studies have examined solar influences on the middle atmosphere. *Hood and Zhou* [1999] found that observed total column ozone response to UV rotational variations was consistent with model predictions, and was also similar between the maxima of solar cycles 21 and 22. *Zhou et al.* [2000] also found agreement between solar maxima for the stratospheric profile ozone response to short-term UV variations. *Chandra et al.* [1999] identified a solar cycle signal in tropospheric column ozone that appears to be out of phase with the stratospheric column ozone response. *Callis et al.* [2000] suggested that stratospheric effects of NO_y may explain why the observed ozone sensitivity to solar UV variations at 40 km on solar cycle timescales is a factor of two greater than both predicted long-term ozone response and the observed short-term ozone variations. *Canty and Minschwaner* [2002] observed column OH variations to be correlated with the Mg II index on solar cycle timescales. *van Loon and Shea* [2000] found that temperatures and geopotential heights in the upper troposphere and stratosphere are correlated with the solar cycle, in agreement with model studies by *Arnold and Robinson* [1998] and *Balachandran et al.* [1999]. *Kodera and Kuroda* [2002] suggested that the effects of solar cycle variations are transferred to the lower atmosphere by changing the balance of stratopause circulation between radiatively controlled and

Copyright 2004 by the American Geophysical Union.
0148-0227/04/2003JD004074$09.00

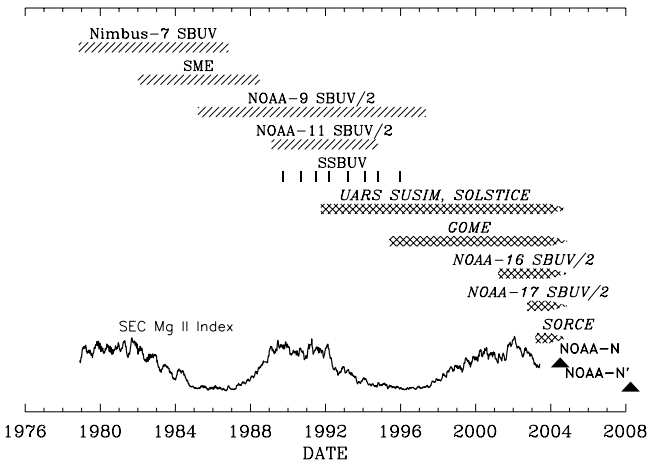

Figure 1. Timeline of satellite solar UV measurements since 1978. The 27-day averaged time series of the NOAA SEC Mg II index time series [*Viereck and Puga*, 1999] is shown for reference.

dynamically controlled states. 2-D model studies show that the effects of volcanic eruptions can complicate the identification of solar cycle-induced ozone variations [*Lee and Smith*, 2003], and can also produce tropospheric temperature changes similar to the combined effects of solar flux and ozone variations [*Haigh*, 1999]. *Khosravi et al.* [2002] modeled mesospheric responses to solar cycle variations, and showed that changes in temperature, ozone, and HO_x are comparable to the overall effect of increases in greenhouse gases since 1850.

[3] Early satellite experiments clearly identified UV irradiance variations with an approximate 27-day period [*Heath*, 1969; *Prag and Morse*, 1970], caused by rotation of active regions across the solar disk. Extended measurements in the 1970s suggested that long-term UV irradiance variations were also present, but these measurements differed considerably in estimates of magnitude and spectral dependence [*Smith and Gottlieb*, 1974; *Heath and Thekaekara*, 1977]. Figure 1 shows that since 1978, a number of different satellite instruments have made continuous solar observations over most of the 120–400 nm wavelength region. Nimbus-7 Solar Backscatter Ultraviolet (SBUV) measured solar activity from solar cycle 21 maximum to the minimum between cycles 21 and 22. Instrument response changes were modeled based on special measurement results from selected periods, but were not measured directly [*Schlesinger and Cebula*, 1992; *DeLand and Cebula*, 2001]. The Solar Mesosphere Explorer (SME) also measured from cycle 21 maximum to the cycle 21–22 minimum. Its long-term calibration was established using multiple solar diffusers and comparisons with rocket underflights [*Rottman*, 1988]. The NOAA-11 SBUV, model 2 (SBUV/2) instrument measured the maximum and declining phase of solar cycle 22. Its long-term calibration utilized an onboard system and comparisons with coincident Shuttle SBUV (SSBUV) measurements from Shuttle flights [*Cebula et al.*, 1998a]. The Upper Atmospheric Research Satellite (UARS) Solar Ultraviolet Spectral Irradiance Monitor (SUSIM) [*Floyd et al.*, 2002] and UARS Solar Stellar Intercomparison Experiment (SOLSTICE) [*Rottman et al.*, 2001] instruments have observed the Sun from the maximum of solar cycle 22 to the maximum of solar cycle 23. SUSIM uses multiple gratings, filters, and detectors in different combinations with onboard deuterium lamps to determine instrument response changes. SOLSTICE observes an ensemble of young blue-white stars to monitor instrument response changes. Both instruments employ on-orbit calibration methods to track long-term variations in instrument performance and produce fully calibrated irradiance data. The Global Ozone Monitoring Instrument (GOME) [*Weber et al.*, 1998] has made measurements from the minimum of solar cycle 22 to the present. However, the GOME solar irradiance data do not yet have a long-term calibration.

[4] The NOAA-9 SBUV/2 instrument was the first in a series of eight instruments designed to continue the Nimbus-7 SBUV ozone and solar measurements from NOAA operational spacecraft. NOAA-9 measured solar spectral UV irradiance from March 1985 to May 1997, providing the first solar irradiance data set covering a complete solar cycle from one minimum to the next. Previous work has examined short-term solar variability during solar minima from the uncorrected NOAA-9 irradiance data [*DeLand and Cebula*, 1998a]. This paper describes the creation of a fully calibrated irradiance data set for NOAA-9 SBUV/2. The primary method used to derive the long-term instrument characterization is a series of comparisons with solar irradiance data from coincident Shuttle SBUV (SSBUV) flights between 1989 and 1996. We find that sensitivity corrections are spectrally dependent, ranging from 3–7% at wavelengths longer than 300 nm to ~20% at 190–210 nm. Estimates of solar cycle amplitude at different UV wavelengths are compared with results from other instruments for the three solar cycles observed to date. The NOAA-9 SBUV/2 data set includes the solar activity minima of cycles 21 and 22, and thus provides an opportunity to evaluate possible solar UV irradiance variations arising from the long-term trend in total solar irradiance between solar minima proposed by *Willson and Mordvinov* [2003]. We find no evidence for spectral irradiance changes between solar minima, which is inconsistent with the *Willson and Mordvinov* [2003] result if TSI changes over this time period are linearly correlated with solar UV changes. The calibrated NOAA-9 data provide the final component needed as input to produce a continuous 25-year data set of solar UV irradiance between 170 and 400 nm.

2. Instrument Description

[5] The SBUV/2 instrument is a nadir-viewing Ebert-Fastie double monochromator that covers the wavelength range 160–406 nm with a 1.1 nm bandpass [*Frederick et al.*, 1986]. The primary purpose of the instrument is to measure the stratospheric profile and total column amount of ozone, using wavelengths between 252 and 340 nm. Normal ozone operations are conducted in discrete mode, sequentially collecting samples at 12 wavelengths with a 1.25 second integration time during each 32 second scan. SBUV/2 instruments are flown on NOAA polar-orbiting spacecraft in Sun-synchronous orbits, typically with afternoon Equator-crossing times. Solar irradiance measure-

ments are made by deploying a diffuser plate when the spacecraft crosses the day-night terminator. The SBUV/2 instrument is required to accurately measure signals varying over more than six orders of magnitude. This is accomplished using three separate gain ranges, each with an amplification of approximately 100 relative to the next range. Each gain range slightly overlaps the next, so that there are narrow regions of signal level where range 1 and range 2 (or ranges 2 and 3) measurements are simultaneously valid. The fundamental quantity required for ozone determination is the directional albedo, defined as the ratio of the backscattered radiance I_λ to the incident irradiance F_λ for π units of solar flux. Most calibration parameters cancel out in the calculation of the directional albedo. The only optical element not common to both radiance and irradiance measurements is the solar diffuser, so that careful monitoring of diffuser changes is critical to the creation of accurate ozone values. Each SBUV/2 instrument carries an onboard calibration system to track long-term changes in diffuser reflectivity [*Weiss et al.*, 1991]. Continuous scan (sweep mode) measurements can also be performed, with 0.1 second samples taken at approximate 0.147 nm intervals over the full wavelength range (160–406 nm). Each sweep scan takes 168 s, moving from long to short wavelengths, with an additional 24 s allotted for grating drive retrace and electronic calibration tests. NOAA-9 sweep solar measurements were normally performed for two consecutive scans on one orbit per day. A typical SBUV/2 sweep mode solar spectrum is shown in the work of *DeLand and Cebula* [1998b, Figure 2].

2.1. Instrument Equation

[6] Numerous correction terms are required to convert the observed instrument counts to solar irradiance values. These corrections include electronic offset, photomultiplier tube (PMT) temperature and gain dependence, response nonlinearity, diffuser angular response (goniometry), diffuser reflectivity change, and prelaunch instrument responsivity. Extensive discussions of the data correction terms for SBUV/2 instruments are given in the work of *Hilsenrath et al.* [1995] and *Cebula et al.* [1998a]. We use the term "internally corrected solar data" to describe measurements which have been processed with these corrections, but no correction for long-term throughput change. Following *Cebula et al.* [1998a], the equation for internally corrected solar data can be written as:

$$C = (S - D)NT_{\mathrm{Corr}}\,G\,R\,A\,f_{\mathrm{Diff}}f_{\mathrm{AU}}, \qquad (1)$$

where

$C(\lambda, t)$	internally corrected solar data [mW m^{-2} nm^{-1}];
$S(r, t)$	raw signal [counts]; r = gain range;
$D(r, t)$	electronic offset [counts];
$N(r, S)$	nonlinearity correction;
$T_{\mathrm{Corr}}(r, t)$	PMT temperature correction;
$G(r, \lambda, t)$	interrange ratio;
$R(\lambda)$	initial instrument responsivity [mW m^{-2} nm^{-1} count^{-1}];
$A(\lambda, \alpha, \beta)$	goniometric correction;
$f_{\mathrm{Diff}}(\lambda, t)$	diffuser reflectivity correction;
$f_{\mathrm{AU}}(t)$	solar distance correction (to 1 AU).

Brief descriptions of the time-dependent correction terms are given below.

2.1.1. Electronic Offset D(r, t)

[7] This quantity is introduced into the data stream to avoid counter underflow due to statistical fluctuations at low signal levels. Long-term variations of the offset value for each gain range are tracked separately using night side data. Range 1 offset data were found to require a time-dependent correction, with a 1–2% effect on sweep solar data shortward of ~180 nm. Range 2 and range 3 offset data show negligible time-dependent changes.

2.1.2. PMT Temperature $T_{\mathrm{Corr}}(r, t)$

[8] The SBUV/2 radiometric sensitivity is temperature-dependent for gain range 1 and 2 data, which are measured from the PMT anode. The sensitivity is characterized prelaunch using the PMT temperature, and corrected for all inflight measurements based on concurrent instrument telemetry. Laboratory radiometric calibrations were performed at a nominal PMT temperature of 20°C. The sensitivity correction is approximately +2% for a typical NOAA-9 operating temperature of 10°C. Seasonal fluctuations of ±0.5% were observed due to an annual temperature variation of ±3°C. These fluctuations increased to ±2% as NOAA-9 drifted through a near-terminator orbit, but no long-term effect was observed [*Ahmad et al.*, 1994].

2.1.3. Interrange Ratio $G(r, \lambda, t)$

[9] Discrete mode measurements record data in all three gain ranges simultaneously, enabling in-orbit tracking of the gain ratios. Range 1 (the most sensitive) and range 2 are both measured from the PMT anode, so that the gain between these ranges (IRR_{12}) is simply an electronic amplification factor. We expect IRR_{12} to be constant in wavelength and time, and this is confirmed by the results of *DeLand et al.* [2001]. Range 3 data are measured from the PMT cathode, so that the gain between these ranges (IRR_{23}) incorporates differences between the anode and cathode relationship. IRR_{23} is spectrally dependent, and drifted by approximately 10% during the NOAA-9 lifetime, with 2–4% fluctuations during near-terminator orbit conditions. A full discussion of the procedure used to derive $\mathrm{IRR}_{23}(t)$ is presented in the work of *DeLand et al.* [2001].

2.1.4. Goniometric Correction $A(\lambda, \alpha, \beta)$

[10] The SBUV/2 solar diffuser is a ground aluminum plate that deploys to an angle 28° below the spacecraft horizontal plane. The incoming solar ray thus has an incidence angle of 62° at the start of the measurement period, increasing to ~80° during the two scan measurement sequence. The solar diffuser plate response has an angular dependence that is characterized as a function of spacecraft-centered elevation and azimuth angles. The elevation angle [α] of the solar vector relative to the tangent plane with Earth's surface varies rapidly during each scan (approximately 1° every 20 s) as the spacecraft passes the day-night terminator. The azimuth angle [β], representing the angle between the solar vector and due North, has a seasonal variation, and also experiences long-term changes as the nominal orbit drifts to later Equator-crossing times. The goniometric correction is therefore implicitly time-dependent. Prelaunch measurements determined the goniometric response of the diffuser over a wide range of elevation and azimuth angles. Figure 2 shows that the NOAA-9 orbit drift led to azimuth angles outside the

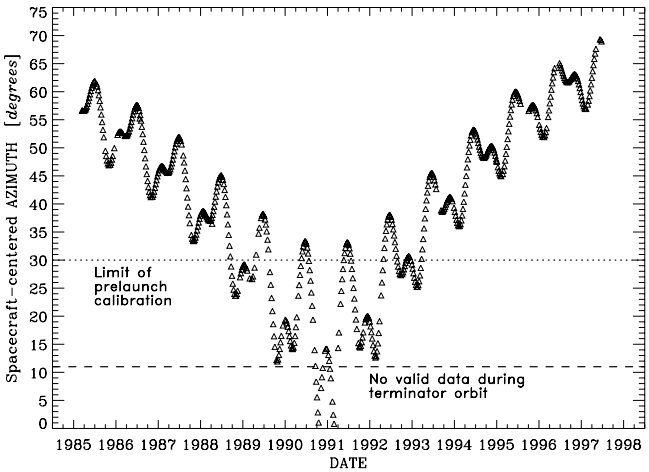

Figure 2. Time series of NOAA-9 spacecraft-centered azimuth angle. Note that the prelaunch goniometric calibration covered the range $\beta = 30-86°$.

prelaunch calibration range during large parts of 1989–1992. A revised goniometric correction was derived from inflight data using the method described in the work of *Hilsenrath et al.* [1995]. However, some NOAA-9 SBUV/2 solar data were unusable because the diffuser was completely shadowed at $\beta < 11°$. A wavelength-dependent goniometric correction term is also required for data at $\lambda < 250$ nm to properly represent non-Lambertian scattering effects.

2.1.5. Diffuser Reflectivity $f_{Diff}(\lambda, t)$

[11] SBUV/2 instruments carry an onboard Hg lamp-based calibration system to track relative changes in diffuser reflectivity [*Weiss et al.*, 1991]. On NOAA-9, this system suffered from significant short-term instabilities, rendering the calibration data useless [*Frederick et al.*, 1986]. A period of increased frequency solar measurements was conducted in mid-1986 to provide a snapshot of diffuser reflectivity changes. This alternate calibration approach is discussed in section 3.1.

2.2. Instrument Operations

[12] NOAA-9 SBUV/2 was launched on 30 December 1984 and operated successfully from its initial Earth view measurements on 10 February 1985 until the sweep solar measurements were terminated on 6 May 1997. There are some gaps in the available solar data record due to occasional shadowing of the solar diffuser and spacecraft anomalies such as safe mode events. Table 1 lists all periods with data gaps greater than 10 days. Other instrument operations effects do not cause complete loss of irradiance data, but require correction in order to create the best product.

2.2.1. Diffuser Deployment

[13] The NOAA-9 solar diffuser occasionally deployed to a position 0.25° greater than its nominal deployment angle. This error leads to an irradiance increase of 0.8–1.3% at the high incidence angles used for SBUV/2 irradiance measurements ($\theta = 60-82°$). Diffuser deployment errors do not trigger a flag in the instrument housekeeping data, and must be identified by inspection of irradiance data at long wavelengths. These errors were corrected on a scan-by-scan basis in the final data set.

2.2.2. Goniometry at High Azimuth Angles

[14] The NOAA-9 spacecraft experienced high spacecraft azimuth angles ($\beta > 57°$) during mid-1985, as shown in Figure 2. On many dates during this period, the derived solar irradiance data fluctuated by as much as 5–6% after the nominal goniometric correction was applied, in a manner consistent with partial shadowing of the solar diffuser. While the elevation and azimuth angle values were within the prelaunch calibration range at this time, unforeseen effects can occur after an instrument is integrated onto the spacecraft. We believe that scattering from an object such as a spacecraft antenna, which was not identified as a problem in prelaunch engineering studies, may have been responsible for these errors. Correction functions for affected data were derived using concurrent data from the SBUV/2 cloud cover radiometer (CCR) when viewing the Sun, which collects coincident data at 378.6 nm using a 1 second cadence. However, some azimuth angle-dependent errors up to 2% are still present. The monochromator and CCR are approximately coaligned, but view slightly different regions of the solar diffuser plate, which might explain these errors. Similar but less frequent problems were observed during 1995–1997, when high azimuth angles appeared again.

2.2.3. Scan 1 Measurement Range

[15] Due to problems with the software controlling the SBUV/2 grating drive, the first two major frames of data (361–406 nm) from the first scan of each NOAA-9 measurement sequence are unavailable. The prelaunch radiometric calibration is only valid to 400 nm, so that a typical NOAA-9 daily spectrum therefore represents only one sample in the wavelength range 361–400 nm rather than the normal two samples. This problem was corrected for all subsequent SBUV/2 instruments.

2.2.4. Grating Drive Sticking

[16] Late in its lifetime, NOAA-9 began to experience occasional sticking of the grating drive. In sweep mode, this problem typically appeared at wavelengths shortward of 250 nm. The condition usually lasted only a few seconds,

Table 1. NOAA-9 SBUV/2 Solar Data Gaps (10 Days or More)

Missing Data Period	Comment
13 Sept. to 13 Nov. 1988	spacecraft solar array shadowing
19 Sept. to 22 Nov. 1990	diffuser shadowing (low azimuth angle)
21 Jan. to 28 Feb. 1991	diffuser shadowing (low azimuth angle)
1–31 March 1991	no data (file lost)
1–31 Aug. 1993	no data (instrument shut down, NOAA-13 launch)
1 Aug. to 15 Sept. 1995	no data (instrument safe mode/restart)
22 May to 18 June 1996	no data (error in ground processing software)

but in severe cases, all data shortward of the sticking point were lost until the grating drive retraced to its starting position. A listing of dates with complete data loss is provided with the final data set.

3. Time-Dependent Instrument Characterization

[17] Numerous aspects of the NOAA-9 SBUV/2 instrument characterization changed during its lifetime, requiring derivation of corrections to the prelaunch calibration. The sweep mode grating drive performance changed in space, causing the nominal wavelength scale to drift by approximately −0.10 nm from 1985 to 1997. The change in wavelength scale was evaluated by fitting absorption lines in the observed solar spectrum to derive a nominal line center position. The absolute position may differ from reference values due to instrument resolution, but the time-dependent variation of these values indicates the instrument behavior. A similar procedure was used for SSBUV [*Cebula et al.*, 1996a], Nimbus-7 SBUV [*DeLand and Cebula*, 2001], and NOAA-11 SBUV/2 [*Cebula et al.*, 1998a]. We derived a power law time dependence fit to these difference data for 14 absorption lines covering the SBUV/2 spectral range, similar to *Cebula et al.* [1998a, Figure 2]. The fit coefficients derived for the Ca II K line at 393.4 nm were adopted to calculate adjustment values for each daily spectrum. The RMS difference between the Ca II K data and the power law fit is 0.022 nm, which is comparable to the accuracy of the prelaunch wavelength calibration. *DeLand and Cebula* [2001] showed that the results of this method were consistent over the spectral range of Nimbus-7 SBUV.

3.1. Accelerated Diffuser Deployment

[18] The NOAA-9 SBUV/2 onboard calibration system developed significant mercury lamp stability problems shortly after launch, with intensity fluctuations of ±10% during a single sequence [*Frederick et al.*, 1986]. This problem prevented the use of the system to track diffuser reflectivity changes. In the absence of an onboard calibration system, a period of accelerated diffuser deployment was used to quantify instrument response changes due to diffuser degradation. During a 2-month period in summer 1986, sweep mode solar measurements were performed on every orbit (13–14 times per day), increasing the diffuser exposure rate by a factor of 10. If the diffuser reflectivity change is assumed to be proportional to diffuser exposure, then a multiple linear regression fit to irradiance around this period allows the separation of exposure-dependent and time-dependent response changes. This procedure was used four times for Nimbus-7 SBUV, and successfully characterized most response changes [*Schlesinger and Cebula*, 1992]. NOAA-9 SBUV/2 had only one accelerated deployment period early in its lifetime, and analysis of total ozone data indicates that the actual diffuser behavior began to diverge from predictions after 1992 [*Taylor et al.*, 2003]. *Schlesinger and Cebula* [1992] observed time-dependent changes in the Nimbus-7 diffuser exposure coefficients by virtue of having multiple accelerated deployment periods available. We have applied the accelerated deployment diffuser degradation correction to all NOAA-9 solar data in order to remove the downward step in irradiance associated with the summer 1986 measurements. This correction also reduces the magnitude of the remaining uncorrected instrument throughput change in the irradiance data. The diffuser degradation correction is small at long wavelengths (1% or less at the end of the data record for 330–400 nm), but increases to 10% at 250 nm before decreasing again at shorter wavelengths.

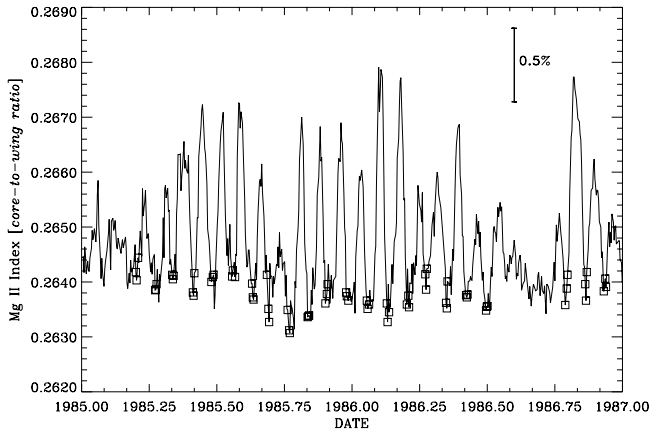

Figure 3. Nimbus-7 SBUV Mg II index values for 1985–1986. Squares indicate dates used for NOAA-9 SBUV/2 solar minimum sensitivity change analysis.

[19] Since the SBUV/2 instrument onboard calibration system does not monitor spectrometer throughput change, additional comparisons are required. A combination of techniques was applied to determine the NOAA-9 time-dependent instrument characterization. Section 3.2 describes the use of low solar activity levels to derive response changes for limited periods in 1985–1986 and 1996–1997. Section 3.3 describes the primary long-term calibration technique, comparisons with concurrent Shuttle SBUV (SSBUV) solar measurements. These techniques also remove any residual errors associated with changes in diffuser degradation coefficients during the later part of the NOAA-9 data record.

3.2. Solar Minimum Analysis

[20] Determination of NOAA-9 SBUV/2 instrument throughput changes using internally corrected data requires the identification of reference irradiance values, either internal or external, for comparison. Since the SSBUV irradiance data are not available during 1985–1988, an alternate approach is required to characterize this period. We chose to take advantage of the low levels of solar activity during solar minimum conditions (e.g., 1985–1986, 1996–1997). The Mg II index core-to-wing ratio is a good indicator of solar UV activity on both solar rotational and solar cycle timescales [*Heath and Schlesinger*, 1986]. The rotational minimum values of the Nimbus-7 SBUV Mg II index varied by less than 0.5% during the 1985–1986 solar minimum period, as shown in Figure 3. This implies a very constant level of solar activity for these dates, compared with the approximate 9% solar cycle variation in the Mg II index. We also calculated the estimated irradiance changes due to solar UV activity between each rotational minimum relative to the first rotation used in 1985, using the Nimbus-7 Mg II index and the scale factors listed in the work of

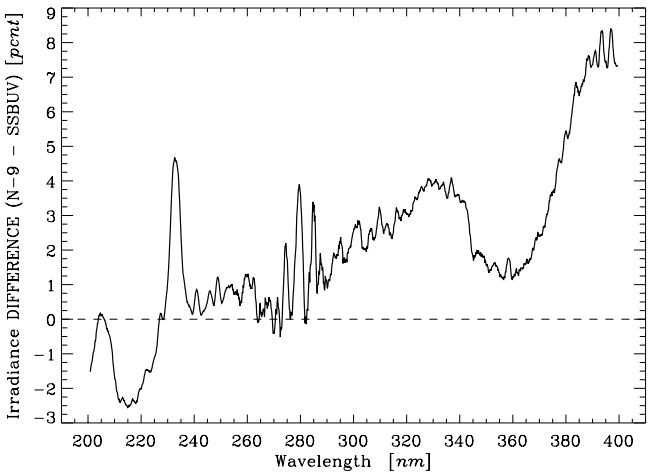

Figure 4. Difference between NOAA-9 initial on-orbit sweep mode solar measurements (March 1985) and flight-averaged solar data from SSBUV-8 (January 1996). Adjusted for the difference in solar activity between dates using predicted variation from Mg II index and scale factors.

DeLand and Cebula [1993]. These adjustments are very small for the dates selected, typically 0.2–0.4% for 170–207 nm and 0.2% or less for longer wavelengths.

[21] Twenty-two (22) rotational minima during 1985–1986 were used in our analysis. We corrected the irradiance data using the diffuser degradation function discussed in section 3.1. Short-term irradiance variations between individual rotations were removed using Mg II index predictions. We then assumed that the remaining time-dependent variation during 1985–1986 represents instrument throughput change. The derived response changes for this period are approximately linear with time, varying from −8% over two years at 200 nm to < 1% longward of 370 nm. The same method was used to constrain NOAA-9 response changes after the last SSBUV flight in January 1996 (see section 3.3). Ten solar rotation minima were selected during the period August 1996 to May 1997 to apply this method. For this short period, derived instrument response changes do not show time-dependent sensitivity changes. The magnitude of the instrument response changes is consistent with the SSBUV-8 coincident ratio results from January 1996 (see section 3.3).

3.3. SSBUV Comparisons

[22] The engineering model of the SBUV/2 instrument was reconfigured to operate on the Space Shuttle, and flew eight missions between 1989 and 1996. The purpose of these SSBUV flights was to provide intercomparison and calibration reference data for on-orbit SBUV/2 instruments [*Hilsenrath et al.*, 1988]. Extensive radiometric calibrations were performed before, during, and after each SSBUV mission, providing accurate corrections for all measurements. A description of the use of SSBUV ozone data for correction of SBUV/2 ozone products is given by *Hilsenrath et al.* [1995]. Comparisons of flight-averaged SSBUV solar spectra show flight-to-flight agreement within 1% [*Cebula et al.*, 1998b]. We have used coincident NOAA-9 and SSBUV solar measurements to evaluate NOAA-9 throughput changes during 1989–1996, following the procedure of *Cebula et al.* [1998a] that was developed for NOAA-11 SBUV/2. Full details of the method are discussed in the work of *Cebula et al.* [1998a], and only a brief summary is given here. The absolute sensitivity difference between NOAA-9 and SSBUV was determined using initial NOAA-9 data from March 1985 (Figure 4). The magnitude and spectral dependence of this difference are comparable to the NOAA-11 sensitivity difference shown in the work of *Cebula et al.* [1998a]. The SSBUV solar irradiance data agree with other coincident irradiance measurements to ±2% or better, as demonstrated in the work of *Cebula et al.* [1996b] and *Woods et al.* [1996]. Therefore, we assume that the majority of the variation in Figure 4 represents NOAA-9 absolute calibration errors. The structure at the Mg II and Ca II absorption features indicates localized wavelength scale differences at the 0.02 nm level. The peak at 232 nm is caused by a Wood's anomaly in the NOAA-9 SBUV/2 grating [*Fowler*, 1993]. Using temporally coincident NOAA-9 and SSBUV data at later dates removes possible errors due to solar activity variations between dates. The SSBUV data were normalized to flight 8 irradiance values at 400 nm. This adjustment was typically ±0.5% or less. SSBUV-1 data between 210 and 270 nm were increased by 1–2% for consistency with SSBUV-2 and SSBUV-3, which had the same level of solar activity. Exact NOAA-9 coincidence data were not available for the SSBUV-1 (October 1989) and SSBUV-2 (October 1990) flights due to NOAA-9 shadowing problems. We replaced these data with NOAA-9 measurements from approximately 27 days before SSBUV-1 and 54 days after the SSBUV-2 flight date, using the same phase of the solar rotation to minimize differences in solar activity. The Mg II index change between the SSBUV flight dates and the selected NOAA-9 dates was 1%. We calculated an irradiance correction using the scale factors to adjust the NOAA-9 data to the SSBUV date. The scale factors listed in the work of *DeLand and Cebula* [1993] have small uncertainties in the wavelength range 210–255 nm, with typical values of 0.50(±0.03) for a 1% change in the Mg II index. We therefore assign an uncertainty of 0.1% at $\lambda > 210$ nm to the temporal adjustment for SSBUV-1 and SSBUV-2 comparisons. The ratio of coincident NOAA-9 and SSBUV spectra, normalized by the initial calibration difference, then gives the relative NOAA-9 response for the date of each Shuttle flight.

[23] Figure 5 shows the spectral dependence of these NOAA-9 response values for three selected SSBUV flights. Notice that dividing out the initial NOAA-9/SSBUV sensitivity difference from Figure 4 yields a smooth and fairly simple spectral dependence for the NOAA-9 degradation curve for each flight. The SSBUV radiometric calibration only covers the wavelength range 200–406 nm. Therefore, another technique is required to derive a sensitivity correction for the NOAA-9 data in the 170–200 nm region. We have chosen to use time series of NOAA-9 irradiance data at 5 nm intervals between 170 and 210 nm to represent the instrument response change, where solar activity variations have been estimated using the Mg II index model and subtracted from the observations. This technique was also used by *Cebula et al.* [1998a] to derive sensitivity correc-

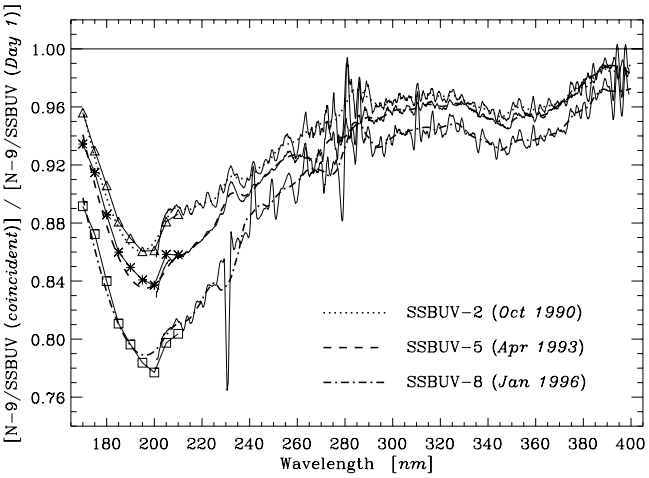

Figure 5. Ratio between NOAA-9 SBUV/2 and SSBUV flight-averaged solar spectra for dates of three SSBUV flights: 2 (October 1990), 5 (April 1993), and 8 (January 1996). All ratios were corrected for initial absolute calibration differences using results from Figure 4. The symbols plotted between 170 and 210 nm represent sensitivity change at each date estimated from time series data, as discussed in the text.

tions at 170–200 nm for the NOAA-11 SBUV/2 data. *Cebula et al.* [1998a] note that this approach makes the assumption that the Mg II-based prediction is reasonably close to the actual long-term solar variation. The close agreement between the 200–210 nm time series values shown in Figure 5 and the SSBUV ratio values for the same dates supports this assumption. Although the method described here is somewhat circular, we feel that it provides the best available correction for the NOAA-9 short wavelength data. Users are nevertheless cautioned as to the possible limitations of the results for determining long-term solar variations between 170 and 200 nm. An indication of the accuracy of this technique is shown in section 5, where the results of intercomparisons with other satellite data sets are presented. NOAA-9 irradiance data shortward of 170 nm were found to be too noisy for effective use. Finally, smoothing spline fits (CLOESS) based on loess fitting methods described by *Cleveland and Grosse* [1991] are used to create a smooth representation of the spectrally dependent NOAA-9 response change corresponding to each SSBUV flight.

3.4. Corrected Irradiance Data

[24] The final NOAA-9 SBUV/2 instrument response change function was determined by calculating 5 nm band average time series from the irradiance ratios of sections 3.2 and 3.3, then fitting each time series with the CLOESS spline function. The density of points for each solar minimum period was reduced to avoid introducing unnecessary structure in the spline fits. Figure 6 shows examples of these combined results for four selected wavelength bands. Overall throughput corrections range from 22% at 200–205 nm to 2% at 395–400 nm. Since there are no instrument degradation data points available from December 1986 to October 1989, the time-dependent spline function represents an interpolation across this period. Any instrument response structure similar to the variations during 1990–1993 will therefore not be captured. These spline functions then provide a basis to calculate daily instrument response changes, which are interpolated across the SBUV/2 wavelength range to create a spectrally dependent instrument

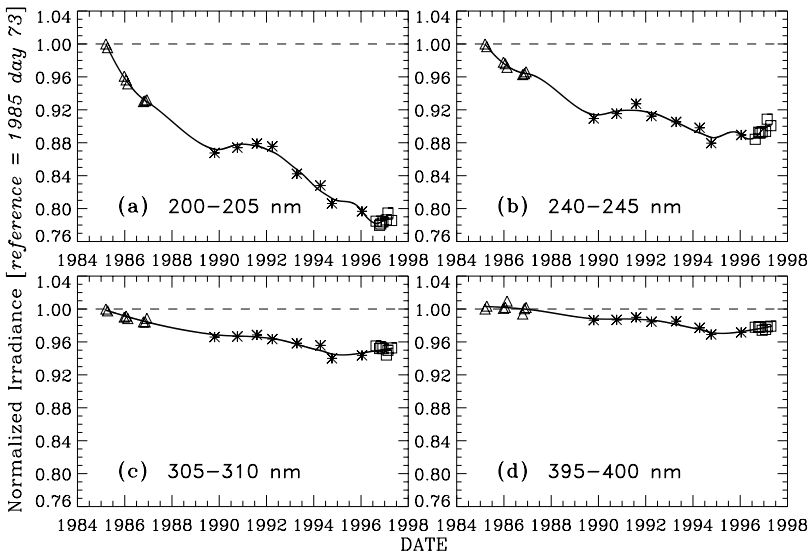

Figure 6. (a) Time series of NOAA-9 internally corrected data averaged between 200 and 205 nm, normalized to the start of measurements. Triangles denote averages during 1985–1986 solar minimum, squares denote averages during 1996–1997 solar minimum, asterisks denote SSBUV ratios, solid line denotes CLOESS fit to data. (b) Time series of NOAA-9 normalized internally corrected data averaged between 240 and 245 nm. Symbols are same as in Figure 6a. (c) Time series of NOAA-9 normalized internally corrected data averaged between 305 and 310 nm. (d) Time series of NOAA-9 normalized internally corrected data averaged between 395 and 400 nm.

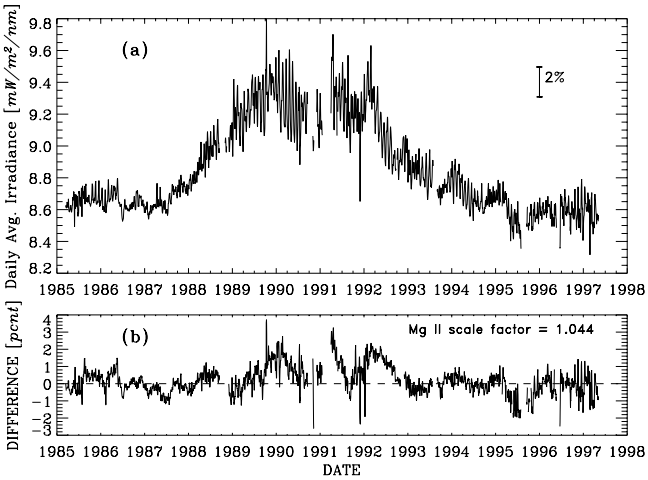

Figure 7. (a) Time series of NOAA-9 SBUV/2 calibrated irradiance data averaged between 200 and 205 nm. A 5-point binomial-weighted average was applied to the data for clarity. (b) Difference between NOAA-9 200–205 nm data and variation predicted by Mg II index and scale factors, normalized to start of data set. A 5-point running average was applied to the residual data for clarity.

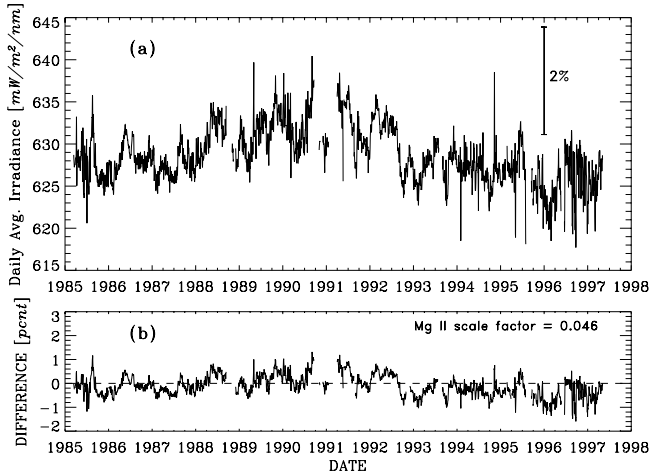

Figure 9. (a) Time series of NOAA-9 SBUV/2 calibrated irradiance data averaged between 305 and 310 nm. A 5-point binomial-weighted average was applied to the data. (b) Difference between NOAA-9 305–310 nm data and variation predicted by Mg II index and scale factors, normalized to start of data set. A 5-point running average was applied to the residual data.

response function corresponding to the date of each measured solar spectrum. The NOAA-9 internally corrected spectral irradiance data were processed using instrument corrections developed with this procedure.

4. Irradiance Results

[25] The corrected NOAA-9 SBUV/2 irradiance data were binned to 1 nm intervals for consistency with other publicly available UV irradiance data sets. Figure 7a shows the time series of these data averaged between 200 and 205 nm. A 5-day binomial-weighted smoothing function has been used to reduce isolated spikes in the plot while preserving the magnitude of rotational variations. SBUV/2 irradiance measurements between 185 and 208 nm have relatively low count levels, and thus are more susceptible to electronic fluctuations caused by charged particle impact on the photomultiplier tube. The solar cycle irradiance variation in Figure 7a is approximately 9.3(±2.3)% from solar minimum in 1986 to the maximum 81-day averaged values in late 1989 and early 1992, where the uncertainty is taken from section 4.1. Rotational modulation variations reached approximately 6% peak-to-peak during solar maximum. The NOAA-9 result is consistent with the Nimbus-7 SBUV estimate of 8.3(±2.6)% for cycle 21 [*DeLand and Cebula*, 2001]. UARS SUSIM observed a range of ~10% at 208 nm for daily values during cycle 22 [*Floyd et al.*, 2002], while UARS SOLSTICE determined an averaged solar cycle variation of 6(±2)% [*Rottman et al.*, 2001]. The lower panel of Figure 7 shows the difference between the NOAA-9 irradiance data and solar variations predicted by the Mg II index and scale factor model. The long-term agreement is generally within ±1%, consistent with the results obtained by *DeLand and Cebula* [1998b] for NOAA-11 SBUV/2. Larger differences are observed in short time periods during 1990–1992. This may reflect problems with the NOAA-9 calibration in near-terminator orbit conditions, but could also indicate an under-prediction of solar cycle-length irradiance variations by the Mg II index model. The RMS of these daily residual values is 0.96%, which includes both instrument noise and differences between the irradiance data and the Mg II index model prediction. Figure 8a shows NOAA-9 data averaged over 245–250 nm. The observed solar cycle variation is approximately 5.7(±1.8)%. This is consistent with the Nimbus-7 SBUV estimate of 4.9(±1.8)% at 240–245 nm for cycle 21. Differences from the Mg II index prediction are ±1% or less. The RMS of the residual

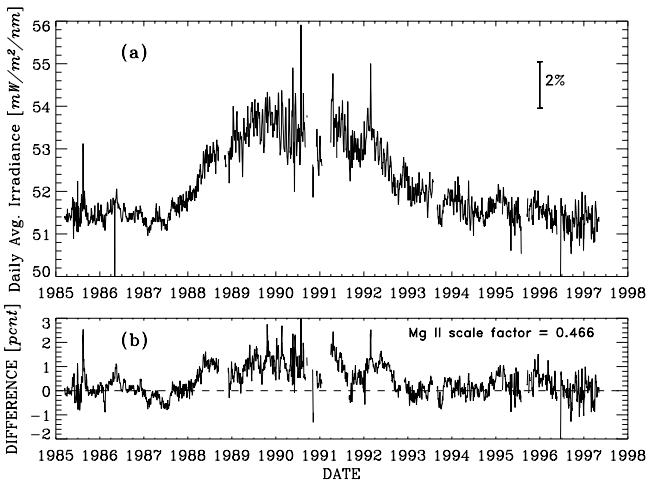

Figure 8. (a) Time series of NOAA-9 SBUV/2 calibrated irradiance data averaged between 245 and 250 nm. A 5-point binomial-weighted average was applied to the data. (b) Difference between NOAA-9 245–255 nm data and variation predicted by Mg II index and scale factors, normalized to start of data set. A 5-point running average was applied to the residual data.

Table 2. NOAA-9 SBUV/2 Time-Dependent Uncertainty Budget[a]

Correction Term	180 nm, %	205 nm, %	250 nm, %	350 nm, %
Thermal sensitivity	0.2	0.2	0.2	—
Diffuser reflectivity	0.2	0.2	0.2	0.2
Interrange ratio IRR_{23}	0.5	0.5	0.5	—
Instrument sensitivity fits	2.0	2.0	1.5	1.0
Wavelength scale correction	0.2	0.3	0.1	0.1
SSBUV repeatability	—	0.9	0.6	0.4
SSBUV normalization	—	0.5	0.5	0.5
Short wavelength characterization	2.0	—	—	—
RSS total	2.9	2.3	1.8	1.2

[a]All uncertainties are ±2σ.

values in Figure 8b is 0.85%. Figure 9a shows NOAA-9 data averaged over 305–310 nm. Variations in these data are ±1% or less. Mg II model estimates of solar variability in this wavelength region were calculated to produce the residual plot in Figure 9b for consistency with Figures 7 and 8. However, the Mg II scale factors are not statistically significant for $\lambda > 285$ nm except for chromospheric emission lines such as Ca II, as shown by *DeLand and Cebula* [1993, Table 2]. A complete treatment of solar variability in this wavelength region requires consideration of sunspot blocking [e.g., *Lean et al.*, 1997]. The RMS residual difference in Figure 9b is 0.54%, representing instrument noise and the accuracy of the NOAA-9 time-dependent sensitivity correction.

4.1. Uncertainty Analysis

[26] *Cebula et al.* [1998a] presented an extensive discussion of absolute and time-dependent uncertainty analysis for NOAA-11 SBUV/2 irradiance data. Since the absolute calibration procedures are very similar between SBUV/2 instruments, we do not repeat that description here. We followed the same approach. The 2σ absolute calibration uncertainties reported for NOAA-11 SBUV/2 are 9.2% at 205 nm, 5.8% at 250 nm, and 3.1% at 350 nm. The actual uncertainty at 205 nm is probably smaller than this value, which includes a "worst case" air-to-vacuum calibration bias term. The NOAA-9 absolute calibration uncertainties are assumed to be approximately the same. Table 2 summarizes terms contributing to the NOAA-9 time-dependent instrument characterization. As noted in section 3.1, errors in the accuracy of the diffuser reflectivity correction are removed by the instrument sensitivity analysis. We adopt 0.2% (2σ) for the uncertainty in this term, following *Cebula et al.* [1998a]. The uncertainty estimate for the time-dependent interrange ratio is 0.5% (2σ). The instrument sensitivity correction uncertainty value reflects the choice of time-dependent CLOESS spline fit tension, because it is difficult to ascertain whether variations between data points at the 0.5–1.0% level are true sensitivity changes or instrument noise. The wavelength scale correction, SSBUV, and short wavelength ($\lambda < 200$ nm) uncertainty values are taken from *Cebula et al.* [1998a]. Combining these terms gives an RSS error estimate of ±1.2% (2σ) for NOAA-9 irradiance data variations at long wavelengths, increasing to ±2.3% for solar cycle variations at 205 nm. Larger uncertainties are appropriate in late 1990 and early 1991, where the goniometric correction is difficult due to the near-terminator orbit.

4.2. Solar Cycle Variability

[27] The NOAA-9 SBUV/2 irradiance data provide a good picture of the spectral dependence of solar cycle variability. Figure 10 shows the spectral dependence of the cycle 22 variation from cycle maximum in June 1989 (average of 27 May to 23 June 1989) to cycle minimum in September 1986 (average of 22 August to 18 September 1986). This variation is consistent with the peak-to-peak irradiance variation for cycle 22 shown by *Floyd et al.* [2002]. The dotted line in Figure 10 shows the predicted irradiance variation between the same time periods calculated using NOAA SEC Mg II index values and 1 nm averaged scale factors. The agreement is within 1%, except for a lower observed irradiance variation at the peak of the Mg II line. This difference is probably due to an inconsistency between irradiance bands in the time-dependent calibration adjustment process. The overall agreement of this result supports the idea that the scale factors, which are derived from short-term irradiance variations, can be successfully used to estimate long-term irradiance variations in the middle ultraviolet.

[28] *Willson and Mordvinov* [2003] have proposed a secular trend in total solar irradiance (TSI) of approximately +0.047%/decade, based on the difference between solar minimum TSI values for cycles 21 and 22. *Lean et al.* [1997] suggest that integrated solar UV variations between 200 and 400 nm represent up to 30% of TSI variations. The observed magnitude of TSI variation from solar cycle minimum to maximum is approximately 0.1% [*Willson*, 1997]. Assuming that the long-term variations of the solar UV irradiance are proportional to the TSI solar cycle changes, the spectral irradiance variation of solar cycle 22 shown in Figure 10 is scaled by a factor of 0.5 to estimate the solar minimum values for cycles 21 and 22 that are based on the TSI long-term trend given by *Willson and Mordvinov* [2003]. This estimate, based on the TSI trend,

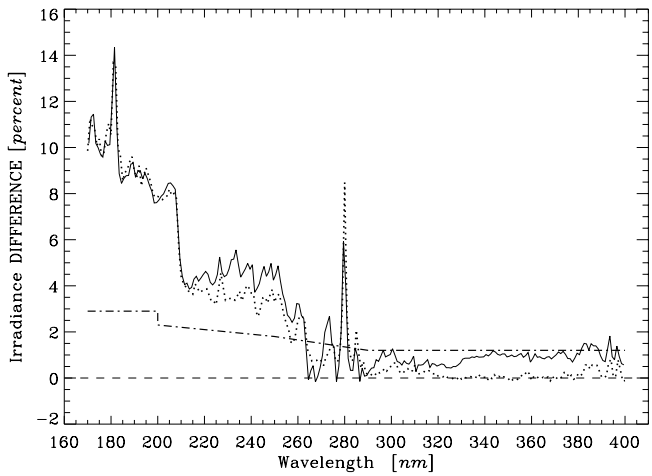

Figure 10. Change in NOAA-9 SBUV/2 spectral irradiance from the maximum to the minimum of solar cycle 22. Dot-dashed line denotes 2σ uncertainty in long-term instrument characterization. Dotted line denotes predicted irradiance variation using Mg II index and scale factors.

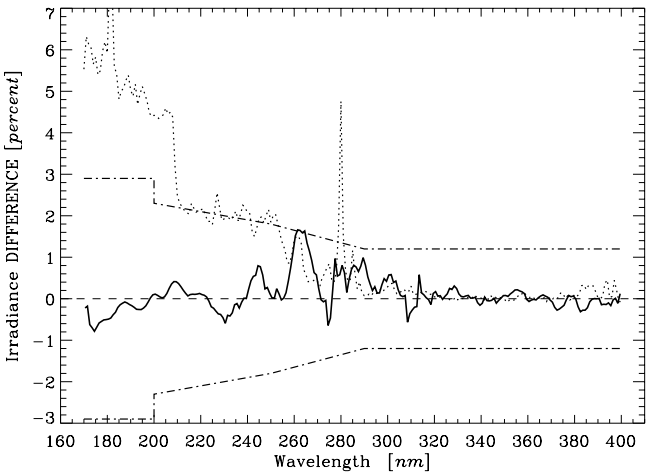

Figure 11. Change in NOAA-9 SBUV/2 spectral irradiance from the minimum of solar cycle 21 to the minimum of solar cycle 22. A 5-point running average was applied for clarity. Dot-dashed line denotes ±2σ uncertainty in long-term instrument characterization. Dotted line denotes predicted irradiance variation based on TSI trend of *Willson and Mordvinov* [2003] and observed spectral dependence for solar cycle variations.

predicts a +4.4% irradiance increase at 200–205 nm and a +2.7% irradiance increase at 245–250 nm between the minima of solar cycles 21 and 22, as shown by the dotted line in Figure 11. The predicted change at 200–205 nm is significantly larger than the NOAA-9 SBUV/2 long-term uncertainty derived in section 4.1. We therefore examined the NOAA-9 SBUV/2 data for UV irradiance variations between solar minima. Approximate dates for the lowest solar activity levels during the solar cycle 21 and 22 minima observed by NOAA-9 are September 1986 and September 1996, respectively [*Harvey and White*, 1999]. We created reference data for each solar minimum period to evaluate possible spectral irradiance changes, averaging a complete solar rotation in each case (22 August to 18 September 1986 for cycle 21; 20 July to 15 August 1996 for cycle 22) to reduce noise. The observed difference between cycle 22 and

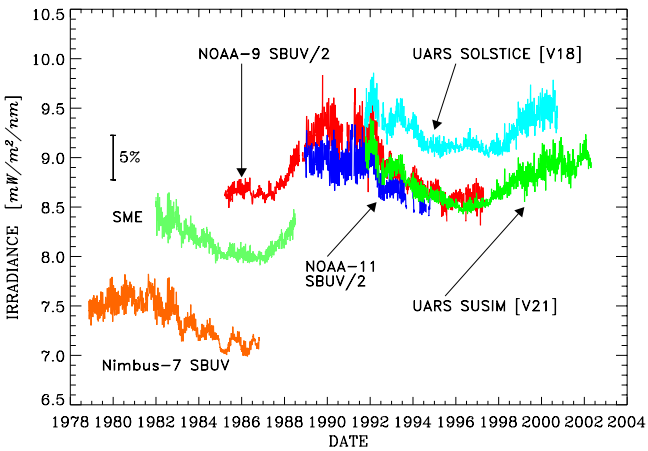

Figure 12. Time series of published solar irradiance data sets at 200–205 nm.

Table 3. Absolute Calibration Uncertainty at 200–205 nm[a]

Instrument	Uncertainty, %	Reference
Nimbus-7 SBUV	10.9	*Schlesinger et al.* [1988]
SME	15	*Rottman* [1988]
NOAA-9 SBUV/2	9.2	this paper
NOAA-11 SBUV/2	9.2	*Cebula et al.* [1998a]
UARS SUSIM	5.3	*Woods et al.* [1996]
UARS SOLSTICE	5	*Woods et al.* [1996]

[a]All uncertainties are ±2σ.

cycle 21 minimum irradiance values is shown by the solid line in Figure 11. The magnitude of the difference is generally ±1% or less, with no clear spectral dependence. There is no evidence for chromospheric irradiance changes between solar minima in the NOAA-9 SBUV/2 data at UV wavelengths within the accuracy of our calibration technique. This conclusion is consistent with the results of *Viereck and Puga* [1999], which are based on Mg II index proxy measurements at the minima of solar cycles 21 and 22. The NOAA-9 SBUV/2 results are not consistent with

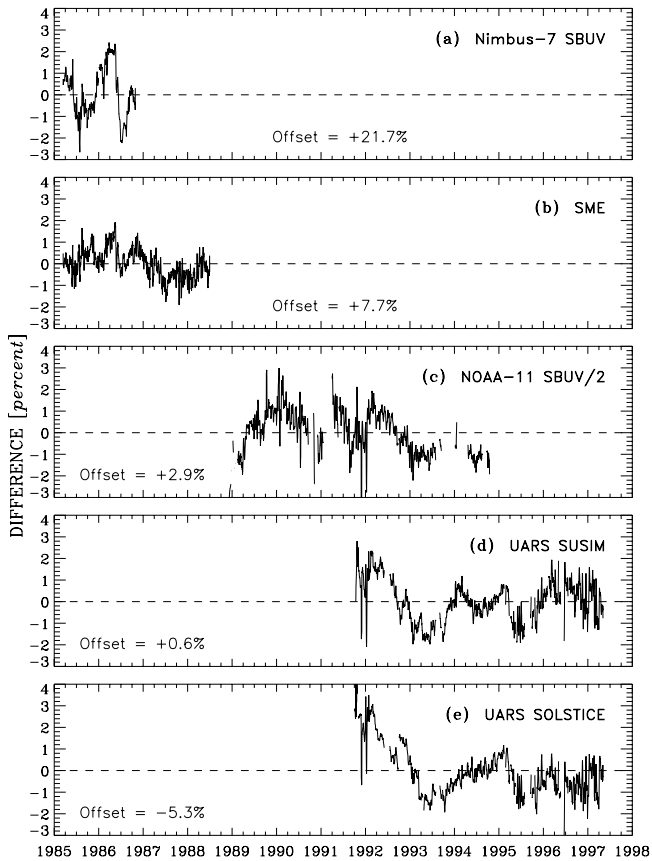

Figure 13. (a) Difference between NOAA-9 SBUV/2 and Nimbus-7 SBUV 200–205 nm data during overlap period. The average bias was removed. (b) Difference between NOAA-9 SBUV/2 and SME 200–205 nm data during overlap period. (c) Difference between NOAA-9 SBUV/2 and NOAA-11 SBUV/2 200–205 nm data during overlap period. (d) Difference between NOAA-9 SBUV/2 and UARS SUSIM 200–205 nm data during overlap period. (e) Difference between NOAA-9 SBUV/2 and UARS SOLSTICE 200–205 nm data during overlap period.

the TSI change derived by *Willson and Mordvinov* [2003] if TSI variations between solar minima are linearly related to UV irradiance variations. We are not able to evaluate the possibility that irradiance changes at visible or near-IR wavelengths may also produce TSI changes between solar minima. Determination of possible long-term variations in photospheric irradiances will require improved instrumental accuracy.

5. Intercomparisons

[29] The timeline in Figure 1 shows that there are many opportunities for intercomparison of NOAA-9 SBUV/2 irradiance data with other satellite instruments. A complete analysis over all wavelengths will be presented at a later date. In this paper, we present comparisons using data averaged between 200 and 205 nm as an illustration because of its significance for stratospheric photochemistry. Figure 12 shows absolute irradiance time series of 200–205 nm data from all published data sets. An initial conclusion from this figure is that, while absolute calibration differences of 5–10% (larger for Nimbus-7 SBUV) exist between different instruments, all data sets reproduce the basic features of observed solar variability (rotational modulation, 11-year cycle). Table 3 lists the published absolute calibration uncertainties at 200–205 nm for each instrument. Figure 13 shows time series of the difference between the NOAA-9 200–205 nm data and each overlapping data set. For each panel, the average bias has been removed to facilitate examination of time-dependent differences. There are no drifts larger than 2% between NOAA-9 SBUV/2 and other satellite instruments over the period of each overlap. Quasi-annual fluctuations in Figure 13a are largely due to periodic variations in Nimbus-7 SBUV data, as discussed by *DeLand and Cebula* [2001]. We believe that the variations during 1992–1993 in Figures 13d and 13e are due to uncorrected NOAA-9 calibration error in this period, as shown in Figure 7b. Other recent multisatellite irradiance comparisons include *DeLand and Cebula* [1998b] (NOAA-11, SUSIM, UARS SOLSTICE), *DeLand and Cebula* [2001] (Nimbus-7, SME), and *DeLand et al.* [2004] (UARS SUSIM, UARS SOLSTICE). Comparisons at other wavelength bands in these papers demonstrate that each satellite has its own spectral and temporal regions with better and worse performance. Taken together, these comparisons provide a realistic estimate of the present long-term uncertainty in solar UV irradiance data sets. An important next step is the creation of a unified spectral irradiance data set covering the period 1978–2002, which requires additional judgments as to which data set to use during intervals with multiple working instruments. We hope to undertake this task in the near future.

6. Conclusion

[30] We have developed a long-term NOAA-9 SBUV/2 solar spectral UV irradiance data set. The instrument characterization used coincidences with Shuttle SBUV measurements to quantify NOAA-9 temporal changes. The long-term characterization for 170–200 nm irradiance data was developed based on Mg II index predictions, and agrees well with SSBUV-based results at 200 nm. The corrected NOAA-9 data provide daily spectra between 170 and 400 nm from March 1985 to May 1997, covering the full range of solar cycle 22. Solar cycle amplitudes determined from these data are consistent with previous results for cycles 21 and 22. The NOAA-9 SBUV/2 irradiance data show no evidence for irradiance changes shortward of 400 nm between the minima of solar cycles 21 and 22 to within the accuracy of our calibration technique. This result is not consistent with the TSI change proposed by *Willson and Mordvinov* [2003] if TSI variations are linearly correlated with UV irradiance variations. The complete NOAA-9 irradiance data set is available at http://ozone.sesda.com/solar/, and will be archived at the National Geophysical Data Center (NGDC). In the near future, we hope to combine these data with other measurements to produce a unified spectral irradiance data set covering 25 years from 1978 to the present.

[31] **Acknowledgments.** This work was supported by NASA contract NAS1-98106. The raw SBUV/2 data were obtained from NOAA/NESDIS with support from the NOAA Climate and Global Change Atmospheric Chemistry Element. Comments from three reviewers provided valuable guidance for improving the manuscript.

References

Ahmad, Z., M. T. DeLand, R. P. Cebula, H. Weiss, C. G. Wellemeyer, W. G. Planet, J. H. Lienesch, H. D. Bowman, A. J. Miller, and R. M. Nagatani (1994), Accuracy of total ozone retrieval from NOAA SBUV/2 measurements: Impact of instrument performance, *J. Geophys. Res.*, *99*, 22,975–22,984.

Arnold, N. F., and T. R. Robinson (1998), Solar cycle changes to planetary wave propagation and their influence on the middle atmosphere circulation, *Ann. Geophys.*, *16*, 69–76.

Balachandran, N. K., D. Rind, P. Lonergan, and D. T. Shindell (1999), Effects of solar cycle variability on the lower stratosphere and the troposphere, *J. Geophys. Res.*, *104*, 27,321–27,339.

Callis, L. B., M. Natarajan, and J. D. Lambeth (2000), Calculated upper stratospheric effects of solar UV flux and NO_y variations during the 11-year solar cycle, *Geophys. Res. Lett.*, *27*, 3869–3872.

Canty, T., and K. Minschwaner (2002), Seasonal and solar cycle variability of OH in the middle atmosphere, *J. Geophys. Res.*, *107*(D24), 4737, doi:10.1029/2002JD002278.

Cebula, R. P., E. Hilsenrath, P. W. DeCamp, K. Laamann, S. Janz, and K. McCullough (1996a), The SSBUV experiment wavelength scale and stability: 1988 to 1994, *Metrologia*, *32*, 633–636.

Cebula, R. P., G. O. Thullier, M. E. VanHoosier, E. Hilsenrath, M. Herse, G. E. Brueckner, and P. C. Simon (1996b), Observations of the solar irradiance in the 200–350 nm interval during the ATLAS-1 mission: A comparison among three sets of measurements-SSBUV, SOLSPEC, and SUSIM, *Geophys. Res. Lett.*, *23*, 2289–2292.

Cebula, R. P., M. T. DeLand, and E. Hilsenrath (1998a), NOAA 11 Solar Backscattered Ultraviolet Model 2 (SBUV/2) instrument solar spectral irradiance measurements in 1989–1994: 1. Observations and long-term calibration, *J. Geophys. Res.*, *103*, 16,235–16,249.

Cebula, R. P., L.-K. Huang, and E. Hilsenrath (1998b), SSBUV sensitivity drift determined using solar spectral irradiance measurements, *Metrologia*, *35*, 677–683.

Chandra, S., J. R. Ziemke, and R. W. Stewart (1999), An 11-year solar cycle in tropospheric ozone from TOMS measurements, *Geophys. Res. Lett.*, *26*, 185–188.

Cleveland, W. S., and E. Grosse (1991), Computational methods for local regression, *Stat. Comput.*, *1*, 47–62.

DeLand, M. T., and R. P. Cebula (1993), Composite Mg II solar activity index for solar cycles 21 and 22, *J. Geophys. Res.*, *98*, 12,809–12,823.

DeLand, M. T., and R. P. Cebula (1998a), Solar UV activity at solar cycle 21 and 22 minimum from NOAA-9 SBUV/2 data, *Sol. Phys.*, *177*, 105–116.

DeLand, M. T., and R. P. Cebula (1998b), NOAA 11 Solar Backscattered Ultraviolet Model 2 (SBUV/2) instrument solar spectral irradiance measurements in 1989–1994: 2. Results, validation, and comparisons, *J. Geophys. Res.*, *103*, 16,251–16,273.

DeLand, M. T., and R. P. Cebula (2001), Spectral solar UV irradiance data for cycle 21, *J. Geophys. Res.*, *106*, 21,569–21,583.

DeLand, M. T., R. P. Cebula, L.-K. Huang, S. L. Taylor, R. S. Stolarski, and R. D. McPeters (2001), Observations of "hysteresis" in backscattered ultraviolet ozone data, *J. Atmos. Oceanic Technol.*, *19*, 914–924.

DeLand, M. T., L. E. Floyd, G. J. Rottman, and J. M. Pap (2004), Status of UARS solar UV irradiance data, *Adv. Space Res*, in press.

Floyd, L. E., D. K. Prinz, P. C. Crane, and L. C. Herring (2002), Solar UV irradiance variation during cycles 22 and 23, *Adv. Space Res.*, *29*, 1957–1962.

Fowler, W. F. (1993), Wood's anomalies in the SBUV/2, *Rep. SBUV-WF-93-721*, 5 pp., Ball Aerosp. Syst. Eng., Boulder, Colo.

Frederick, J. E., R. P. Cebula, and D. F. Heath (1986), Instrument characterization for the detection of long-term changes in stratospheric ozone: An analysis of the SBUV/2 radiometer, *J. Atmos. Oceanic Technol.*, *3*, 472–480.

Haigh, J. D. (1999), Modelling the impact of solar variability on climate, *J. Atmos. Sol. Terr. Phys.*, *61*, 63–72.

Harvey, K. L., and O. R. White (1999), What is solar cycle minimum?, *J. Geophys. Res.*, *104*, 19,759–19,764.

Heath, D. F. (1969), Observations of the intensity and variability of the near ultraviolet solar flux from the Nimbus 3 satellite, *J. Atmos. Sci.*, *26*, 1157–1160.

Heath, D. F., and B. M. Schlesinger (1986), The Mg-280 nm doublet as a monitor of changes in solar ultraviolet irradiance, *J. Geophys. Res.*, *91*, 8672–8682.

Heath, D. F., and M. P. Thekaekara (1977), The solar spectrum between 1200 and 3000 Å, in *The Solar Output and Its Variation*, edited by O. R. White, pp. 193–212, Colo. Assoc. Univ. Press, Boulder, Colo.

Hilsenrath, E., D. Williams, and J. Frederick (1988), Calibration of long term data sets from operational satellites using the Space Shuttle, *SPIE Proc.*, *924*, 215–222.

Hilsenrath, E., R. P. Cebula, M. T. DeLand, K. Laamann, S. Taylor, C. Wellemeyer, and P. K. Bhartia (1995), Calibration of the NOAA 11 solar backscatter ultraviolet (SBUV/2) ozone data set from 1989 to 1993 using in-flight calibration data and SSBUV, *J. Geophys. Res.*, *100*, 1351–1366.

Hood, L. L., and S. Zhou (1999), Stratospheric effects of 27-day solar ultraviolet variations: The column ozone response and comparisons of solar cycles 21 and 22, *J. Geophys. Res.*, *104*, 26,473–26,479.

Khosravi, R., G. Brasseur, A. Smith, D. Rusch, S. Walters, S. Chabrillat, and G. Kockarts (2002), Response of the mesosphere to human-induced perturbations and solar variability calculated by a 2-D model, *J. Geophys. Res.*, *107*(D18), 4358, doi:10.1029/2001JD001235.

Kodera, K., and Y. Kuroda (2002), Dynamical response to the solar cycle, *J. Geophys. Res.*, *107*(D24), 4749, doi:10.1029/2002JD002224.

Lean, J. L., G. J. Rottman, H. L. Kyle, T. N. Woods, J. R. Hickey, and L. C. Puga (1997), Detection and parameterization of variations in solar mid- and near-ultraviolet radiation (200–400 nm), *J. Geophys. Res.*, *102*, 29,939–29,956.

Lee, H., and A. K. Smith (2003), Simulation of the combined effects of solar cycle, quasi-biennal oscillation, and volcanic forcing on stratospheric ozone changes in recent decades, *J. Geophys. Res.*, *108*(D2), 4049, doi:10.1029/2001JD001503.

Meier, R. R. (1991), Ultraviolet spectroscopy and remote sensing of the upper atmosphere, *Space Sci. Rev.*, *58*, 1–185.

Prag, A. B., and F. A. Morse (1970), Variations in the solar ultraviolet flux from July 13 to August 9, 1968, *J. Geophys. Res.*, *75*, 4613–4621.

Rottman, G. J. (1988), Observations of solar UV and EUV variability, *Adv. Space Res.*, *8*(7), 53–66.

Rottman, G., T. Woods, M. Snow, and G. DeToma (2001), The solar cycle variation in ultraviolet irradiance, *Adv. Space Res.*, *27*, 1927–1932.

Schlesinger, B. M., and R. P. Cebula (1992), Solar variation 1979–1987 estimated from an empirical model for changes with time in the sensitivity of the Solar Backscatter Ultraviolet instrument, *J. Geophys. Res.*, *97*, 10,119–10,134.

Schlesinger, B. M., R. P. Cebula, D. F. Heath, and A. J. Fleig (1988), Nimbus-7 Solar Backscatter Ultraviolet (SBUV) spectral scan solar irradiance and Earth Radiance Products user's guide, *NASA Res. Publ. RP-1199*, 74 pp., Greenbelt, Md.

Smith, E. V. P., and D. M. Gottlieb (1974), Solar flux and its variations, *Space Sci. Rev.*, *16*, 771–802.

Taylor, S. L., R. P. Cebula, M. T. DeLand, L.-K. Huang, R. S. Stolarski, and R. D. McPeters (2003), Improved calibration of NOAA-9 and NOAA-11 SBUV/2 total ozone data using in-flight validation methods, *Int. J. Remote Sens.*, *24*, 315–328.

van Loon, H., and D. J. Shea (2000), The global 11-year solar signal in July–August, *Geophys. Res. Lett.*, *27*, 2965–2968.

Viereck, R., and L. C. Puga (1999), The NOAA Mg II core-to-wing solar index: Construction of a 20-year time series of chromospheric variability from multiple satellites, *J. Geophys. Res.*, *104*, 9995–10,005.

Weber, M., J. P. Burrows, and R. P. Cebula (1998), GOME solar UV/VIS irradiance measurements in 1995 and 1996—First results on proxy solar activity studies, *Sol. Phys.*, *177*, 63–77.

Weiss, H., R. P. Cebula, K. Laamann, and R. D. Hudson (1991), Evaluation of the NOAA 11 Solar Backscatter Ultraviolet radiometer, mod 2 (SBUV/2), Inflight calibration, *Proc. SPIE Int. Soc. Opt. Eng.*, *1493*, 80–90.

Willson, R. C. (1997), Total solar irradiance trend during solar cycles 21 and 22, *Science*, *277*, 1963–1965.

Willson, R. C., and A. V. Mordvinov (2003), Secular total solar irradiance trend during solar cycles 21–23, *Geophys. Res. Lett.*, *30*(5), 1199, doi:10.1029/2002GL016038.

Woods, T. N., et al. (1996), Validation of the UARS solar ultraviolet irradiances: Comparisons with the ATLAS 1 and 2 measurements, *J. Geophys. Res.*, *101*, 9541–9569.

Zhou, S., A. J. Miller, and L. L. Hood (2000), A partial correlation analysis of the stratospheric ozone response to 27-day solar UV variations with temperature effect removed, *J. Geophys. Res.*, *105*, 4491–4500.

R. P. Cebula and M. T. DeLand, Science Systems and Applications, Inc. (SSAI), 10210 Greenbelt Road, Suite 400, Lanham, MD 20706, USA. (matthew_deland@ssaihq.com)

E. Hilsenrath, NASA Goddard Space Flight Center, Code 916, Greenbelt, MD 20771, USA.